


## Sync and Swarm: Solvable Model of Nonidentical Swarmalators

S. Yoon<sup>1</sup>, K. P. O’Keeffe<sup>2</sup>, J. F. F. Mendes<sup>1</sup>, and A. V. Goltsev<sup>1</sup>

<sup>1</sup>*Departamento de Física da Universidade de Aveiro and I3N, Campus Universitário de Santiago, 3810-193 Aveiro, Portugal*

<sup>2</sup>*Senseable City Lab, Massachusetts Institute of Technology, Cambridge, Massachusetts 02139, USA*

 (Received 18 March 2022; accepted 13 October 2022; published 10 November 2022)

We study a model of nonidentical swarmalators, generalizations of phase oscillators that both sync in time and swarm in space. The model produces four collective states: asynchrony, sync clusters, vortexlike phase waves, and a mixed state. These states occur in many real-world swarmalator systems such as biological microswimmers, chemical nanomotors, and groups of drones. A generalized Ott-Antonsen ansatz provides the first analytic description of these states and conditions for their existence. We show how this approach may be used in studies of active matter and related disciplines.

DOI: 10.1103/PhysRevLett.129.208002

Synchronization is a universal phenomenon [1–3] seen in coupled lasers [4] and beating heart cells [5]. When in sync, the units of such systems align the rhythms of their oscillations, but do not move through space. Swarming, as in flocks of birds [6] or schools of fish [7], is a sister effect where the roles of space and time are swapped. The units coordinate their movements in space, but do not synchronize an internal oscillation.

The units of some systems coordinate themselves in both space and time concurrently. Japanese tree frogs sync their courting calls as they form packs to attract mates [8,9]. Starfish embryos sync their genetic cycles with their movements creating exotic “living crystals” [10]. Janus particles [11–13], Quincke rollers [14–16], and other driven colloids [17–20] lock their rotations as they self-assemble in space. The emergent “sync-selected” structures have great applied power. They have been used to degrade pollutants [21–24], repair electrical circuits [25], and to shatter blood clots [26,27].

Theoretical studies of systems which mix sync with swarming are on the rise [28–32]. Tanaka *et al.* derived a universal model of chemotactic oscillators with diverse behavior [31,33]. Active matter researchers studied a Vicsek model with self-rotating (synchronizable) units [28,34,35] which imitate various types of colloid. O’Keeffe *et al.* introduced a model of “swarmalators” [29], whose states have been found in the lab and in nature [14,36,37], and is being further studied [38–46].

Analytic results on swarmalators are sparse. Order parameters, bifurcations, etc. are hard to compute given the systems’ nonlinearities and numerous degrees of freedom. Active matter such as the driven colloids mentioned earlier (which may be considered swarmalators) are hard to analyze for the same reasons. The Vicsek model [47], for example, requires an in-depth use of statistical physics tools (dynamical renormalization groups, etc.) to be solved [48]. As for generalized Vicsek models, often only the stability

of the simple incoherent state is analyzed, while order parameters are found purely numerically [28,32,34,35]. As such, easily and exactly solvable models of active matter are somewhat rare.

This Letter shows how this gap in active matter and swarmalator research may begin to be closed using technology from sync studies. We use Kuramoto’s classic self-consistency analysis [2] in hand with a generalized Ott-Antonsen (OA) ansatz [49]—two breakthrough tools—to study swarmalators which run on a 1D ring. This simple model captures the essential aspects of real-world swarmalators and active matter, yet is also solvable: its order parameters and collective states may be characterized exactly. To our knowledge, exact results for the order parameters of an active matter collective are few; in this sense our Letter contributes to this vibrant field.

*Model.*—The model we study is [50]

$$\dot{x}_i = v_i + \frac{J}{N} \sum_{j=1}^N \sin(x_j - x_i) \cos(\theta_j - \theta_i), \quad (1)$$

$$\dot{\theta}_i = \omega_i + \frac{K}{N} \sum_{j=1}^N \sin(\theta_j - \theta_i) \cos(x_j - x_i), \quad (2)$$

where  $(x_i, \theta_i) \in (S^1, S^1)$  are the position and phase of the  $i$ th swarmalator and  $(v_i, \omega_i)$ ,  $(J, K)$  are the associated natural frequencies and couplings. The  $v_i, \omega_i$  are drawn from a Lorentzian distribution,  $g_{v(\omega)}(x) = \Delta_{v(\omega)} / [\pi(x^2 + \Delta_{v(\omega)}^2)]$ , with spreads  $\Delta_v, \Delta_\omega$  and mean set to zero via a change of frame.

The phase dynamics Eq. (2) are a generalized Kuramoto model where it now depends on their pairwise distance  $K_{ij} = K \cos(x_j - x_i)$  [51]. So for  $K > 0$  neighboring swarmalators synchronize more quickly than remote ones (the opposite occurs for  $K < 0$ ). To treat sync and

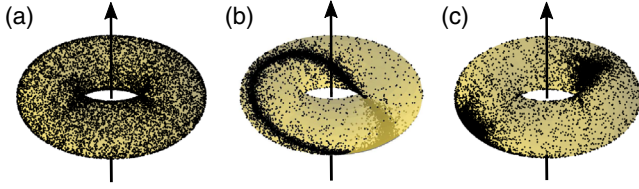


FIG. 1. Steady states of swarmalators (black dots) projected onto the unit torus. Data were generated by integrating Eqs. (1) and (2) with the RK45 solver for  $T = 500$  time units with adaptive step size for  $N = 10^4$  swarmalators with  $\Delta_v = \Delta_\omega = 1$ . (a) Async state for  $(J, K) = (1, 1)$  where swarmalators are uniformly distributed in both space and phase. (b) Phase wave state for  $(J, K) = (1, 40)$  where positions and phases of swarmalators are correlated. (c) Sync state for  $(J, K) = (8, 9)$ , where clusters of swarmalators synced in both space and time coexist with drifting swarmalators.

swarming on the same footing, the space dynamics Eq. (1) are identical to Eq. (2) but with  $x_i$  and  $\theta_i$  switched. Thus for  $J > 0$  synchronized swarmalator's swarm (in the sense of aggregating) more readily than desynchronized ones (the opposite for  $J < 0$ ). In short, the equations model location-dependent synchronization, and phase-dependent aggregation. One can also think of them as sync on the unit torus (Fig. 1) or as the rotational piece of the 2D swarmalator model [52].

Introducing the variables

$$\zeta_i \equiv x_i + \theta_i, \quad \eta_i \equiv x_i - \theta_i, \quad (3)$$

let us write Eqs. (1) and (2) as a pair of linearly coupled Kuramoto models [50]

$$\dot{\zeta}_i = v_i + \omega_i - J_+ S_+ \sin(\zeta_i - \Phi_+) - J_- S_- \sin(\eta_i - \Phi_-), \quad (4)$$

$$\dot{\eta}_i = v_i - \omega_i - J_- S_+ \sin(\zeta_i - \Phi_+) - J_+ S_- \sin(\eta_i - \Phi_-), \quad (5)$$

where  $J_\pm \equiv (J \pm K)/2$  and

$$W_\pm \equiv \frac{1}{N} \sum_{j=1}^N e^{i(x_j \pm \theta_j)} = S_\pm e^{i\Phi_\pm}. \quad (6)$$

These new order parameters measure the systems' space-phase order. When there is perfect correlation between space and phase  $x_i = \pm \theta_i + C$ ,  $S_\pm = 1$ . When  $x_i$  and  $\theta_i$  are uncorrelated,  $S_\pm = 0$ . In a general case ( $J \neq K$ ), the swarmalator and Kuramoto models belong to different classes of collective behavior. The coupling dependence on  $S_\pm$  in Eqs. (4) and (5) leads to new collective states such as a mixed state in which  $S_+$  and  $S_-$  coexist. This state has no analogy in the Kuramoto model.

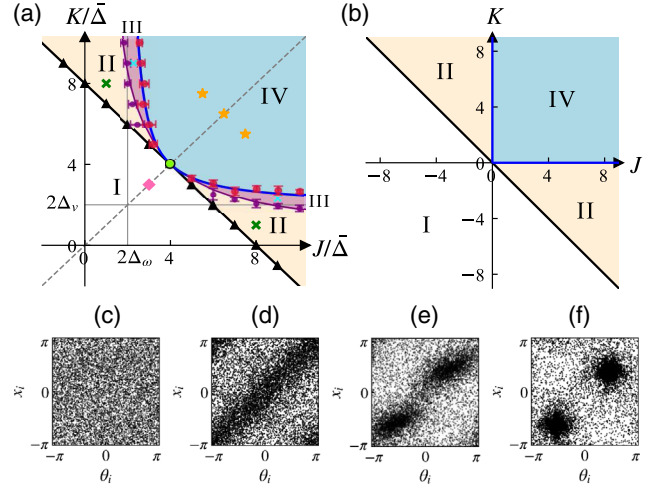


FIG. 2. (a) Phase diagram of the swarmalator model in the  $(J, K)$  plane [in units of  $\bar{\Delta} = (\Delta_v + \Delta_\omega)/2$ ]. Regions I, II, III, and IV correspond to the  $(0,0)$  (async),  $(S,0)/(0,S)$  (phase wave),  $(S_1, S_2)$  (mixed), and  $(S, S)$  (sync) states. The black and blue solid lines represent the critical lines Eqs. (20) and (23). The purple solid line represents the critical line Eq. (S69) in [52]. The black dashed line describes  $J = K$  and the green circle is the tetracritical point. Symbols, black triangles, purple dots, and red circles are critical points found in simulations for  $N = 10^4$ ,  $T = 200$  with adaptive time step RK45 solver, and averaged by 20 realizations. (b) Phase diagram of the model with identical swarmalators (adapted from [50]). (c)–(f) Scatter plots of the  $(0,0)$ ,  $(0, S)$ ,  $(S_1, S_2)$  where  $S_1 < S_2$ , and  $(S, S)$  states in the  $(\theta, x)$  plane. Magenta diamond, green crosses, cyan crosses, and orange stars in panel (a) show the points where we made the scatter plots for (c)–(f), respectively.

Numerics shows the system has four steady states which may be categorised by the pair  $(S_+, S_-)$ . (i) *Async* or  $(0,0)$  state: swarmalators are fully dispersed in space and phase as depicted in Figs. 1(a) and 2(c). There is no space-phase order so  $(S_+, S_-) = (0, 0)$ . (ii) *Phase waves* or  $(S, 0)/(0, S)$  state: swarmalators form a band or phase wave [57] where  $x_i \approx \mp \theta_i$  for  $(S, 0)$  and  $(0, S)$  states, respectively, as depicted in Figs. 1(b) and 2(d). In  $(\zeta, \eta)$  coordinates, swarmalators are partially locked in  $\zeta_i$  and drift in  $\eta_i$ , or vice versa. (iii) Intermediate *mixed* state  $(S_1, S_2)$  with  $S_1 \neq S_2 \neq 0$ , see Fig. 2(e): swarmalators form a band along which clusters of correlated swarmalators are moving. (iv) *Sync* or  $(S, S)$  state: swarmalators are partially locked in both  $\zeta_i$  and  $\eta_i$ . For most initial conditions, two clusters of locked swarmalators separated a distance of  $\pi$  in  $(\zeta, \eta)$  emerge spontaneously, as shown in Figs. 1(c) and 2(f) (single clusters were also observed). This “ $\pi$  state” results from a symmetry in the model: the transformation  $\tilde{x}_i = x_i + \pi$  and  $\tilde{\theta}_i = \theta_i + \pi$  leaves Eqs. (1) and (2) unchanged which means a locked swarmalator can be assigned to either cluster without changing the overall dynamics. The internal symmetry results in the formation of mirrored groups of synchronized swarmalators, see Ref. [52].

Movies of the evolution of these states and demonstrations that they are robust to local coupling (i.e., cutoff beyond a range  $\sigma$ ) are provided in [52].

*Generalized OA ansatz.*—Now we analyze our model by deriving expressions for the order parameters  $W_{\pm}$  in each state. Consider the probability  $f(v, \omega, \zeta, \eta, t)$  to find a swarmalator with natural velocity  $v$ , a natural frequency  $\omega$ , and coordinates  $\zeta$  and  $\eta$  at time  $t$

$$f \equiv \frac{1}{N} \sum_{i=1}^N \delta(v - v_i) \delta(\omega - \omega_i) \delta(\zeta - \zeta_i) \delta(\eta - \eta_i). \quad (7)$$

Differentiating the left and right hand sides of Eq. (7) over  $t$  gives the continuity equation,

$$\begin{aligned} \frac{\partial f}{\partial t} + \frac{\partial}{\partial \zeta} \{ [v + \omega - J_+ S_+ \sin(\zeta - \Phi_+) - J_- S_- \sin(\eta - \Phi_-)] f \} \\ + \frac{\partial}{\partial \eta} \{ [v - \omega - J_- S_+ \sin(\zeta - \Phi_+) - J_+ S_- \sin(\eta - \Phi_-)] f \} = 0. \end{aligned} \quad (8)$$

Ott and Antonsen showed that for the Kuramoto model,  $f$  has an invariant manifold of Poisson kernels (a remarkable finding which effectively solves the model) known as the OA ansatz [49,56]. Since our model is a Kuramoto model on the torus, we search for a “toroidal” OA ansatz: a product of Poisson kernels,

$$\begin{aligned} f(v, \omega, \zeta, \eta, t) = \frac{1}{4\pi^2} g_v(v) g_\omega(\omega) \left[ 1 + \sum_{n=1}^{\infty} \alpha^n e^{in\zeta} + \text{c.c.} \right] \\ \times \left[ 1 + \sum_{m=1}^{\infty} \beta^m e^{im\eta} + \text{c.c.} \right], \end{aligned} \quad (9)$$

where  $\alpha = \alpha(v, \omega, t)$  and  $\beta = \beta(v, \omega, t)$  are unknown functions which must be found self-consistently. Substituting Eq. (9) into Eq. (8) we find that  $f$  satisfies Eq. (8) for all harmonics  $n$  and  $m$  if  $\alpha$  and  $\beta$  satisfy

$$\begin{aligned} \frac{d\alpha}{dt} = -i(v + \omega)\alpha + \frac{1}{2} J_+ (W_+^* - W_+ \alpha^2) \\ + \frac{1}{2} J_- \alpha (W_-^* \beta^* - W_- \beta), \end{aligned} \quad (10)$$

$$\begin{aligned} \frac{d\beta}{dt} = -i(v - \omega)\beta + \frac{1}{2} J_+ (W_-^* - W_- \beta^2) \\ + \frac{1}{2} J_- \beta (W_+^* \alpha^* - W_+ \alpha), \end{aligned} \quad (11)$$

in the submanifold  $\|\alpha\| = \|\beta\| = 1$ . The order parameters  $W_{\pm}$  become

$$W_+ = \int_{-\infty}^{\infty} dv \int_{-\infty}^{\infty} d\omega g_v(v) g_\omega(\omega) \alpha^*(v, \omega, t), \quad (12)$$

$$W_- = \int_{-\infty}^{\infty} dv \int_{-\infty}^{\infty} d\omega g_v(v) g_\omega(\omega) \beta^*(v, \omega, t). \quad (13)$$

Equations (10)–(13) comprise a set of self-consistent equations for  $W_{\pm}$  in the  $N \rightarrow \infty$  limit.

*Analysis of async.*—Here, swarmalators are uniformly distributed in  $x$  and  $\theta$  which corresponds to the trivial fixed point  $W_{\pm} = 0$ . Equations (10) and (11) give  $\alpha = \exp[i(v + \omega)t]$ ,  $\beta = \exp[i(v - \omega)t]$ . Linearizing around  $f = (2\pi)^{-2}$  [52] reveals the state loses stability at

$$J_{+,c} = 2(\Delta_v + \Delta_\omega). \quad (14)$$

Figure 2(a) plots this condition in the  $(J, K)$  plane.

*Analysis of phase waves.*—We analyze the  $(S, 0)$  phase wave state. We look for a solution of Eqs. (10)–(13) that at large time  $t$  satisfies  $\dot{\alpha} = 0$ ,  $\dot{\beta} \neq 0$ ,  $W_+ \neq 0$ , and  $W_- = 0$ . We find

$$\alpha(v, \omega) = H\left(\frac{v + \omega}{S_+ J_+}\right), \quad (15)$$

$$\beta(v, \omega, t) = \exp\left[-i \frac{JK}{J_+} \left(\frac{v}{J} - \frac{\omega}{K}\right) t\right], \quad (16)$$

where we introduced a function

$$H(x) \equiv -ix + \sqrt{1 - x^2}. \quad (17)$$

Equation (16) gives  $W_- = 0$  as desired. Equation (15) implies

$$S_+ = \int_{-\infty}^{\infty} dv \int_{-\infty}^{\infty} d\omega g_v(v) g_\omega(\omega) H^*\left(\frac{v + \omega}{S_+ J_+}\right), \quad (18)$$

where we assume  $\Phi_+ = 0$  without loss of generality due to the rotational symmetry. To compute this integral, first observe that if  $v$  and  $\omega$  are drawn from the Lorentzian distribution, their sum  $v + \omega$  is drawn from a Lorentzian with spread  $\Delta_v + \Delta_\omega$ . Then integrate over  $v + \omega$  using the residue theorem. There is a residue  $i(\Delta_v + \Delta_\omega)$  in the upper half complex plane where  $H^*(x)$  is analytic so  $S_+ = H^*[i(\Delta_v + \Delta_\omega)/S_+ J_+]$ . Thus,

$$S_+ = \left[ 1 - \frac{2(\Delta_v + \Delta_\omega)}{J_+} \right]^{1/2}. \quad (19)$$

We see  $S_+$  bifurcates from 0 at

$$J_{+,c} = \frac{1}{2}(J + K) = 2(\Delta_v + \Delta_\omega) \quad (20)$$

consistent with Eq. (14) as the system transitions from the async to the phase wave state [Fig. 3(a)], see the stability analysis in [52]. The phase wave  $(0, S)$  is a solution of

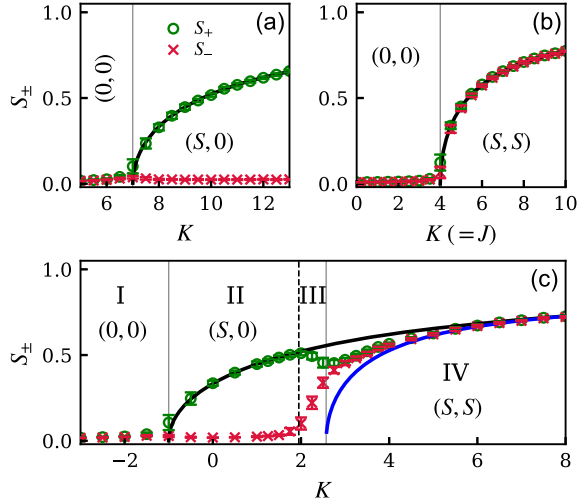


FIG. 3. Order parameters  $S_{\pm}$  versus coupling  $K$ . (a) Async—phase wave transition [region II in Fig. 2(a) at  $J = 1$ ]. (b) Async—sync transition [along the diagonal line in the region IV in Fig. 2(a) at  $J = K$ ]. (c) Async (I), phase wave (II), mixed (III), and sync (IV) states at  $J = 9$ . Black and blue solid lines correspond to theoretical expressions Eqs. (19) and (22), respectively. Black dashed line corresponds to the susceptibility peak, see Ref. [52]. Green open circles and red crosses represent simulation data for the same parameters as in Fig. 2.

Eqs. (10)–(13) that at large time  $t$  satisfies  $\dot{\alpha} \neq 0$ ,  $\dot{\beta} = 0$ ,  $W_+ = 0$ ,  $W_- \neq 0$ .

*Mixed state.*—Here,  $(S_1, S_2)$ , where  $S_1 \neq S_2$ . This state is intermediate between the phase wave and sync states, see Fig. 2(a) and compare Figs. 2(d) and 2(e). The state with either  $S_1 > S_2$  or  $S_1 < S_2$  bifurcates from  $(S, 0)$  or  $(0, S)$ , respectively. The corresponding order parameters and phase boundaries in  $(J, K)$  plane are shown in Figs. 2(a) and 3(c) and discussed in [52]. The special property of the mixed state is that although  $S_1$  and  $S_2$  are time independent, both the functions  $\alpha$  and  $\beta$  are time dependent in contrast to time independent equations (15) and (21) (see below) for the phase wave and the sync states. Analytical properties of  $\alpha$  and  $\beta$  near the boundary with the phase wave are discussed in Sec. IV, see Ref. [52].

*Analysis of sync.*—Here,  $(S_+, S_-) = (S, S)$  so we seek fixed points of Eqs. (10) and (11) with  $W_{\pm} \neq 0$ . We find

$$\alpha(v, \omega) = H \left[ \frac{v}{JS_+} + \frac{\omega}{KS_+} \right], \quad \beta(v, \omega) = H \left[ \frac{v}{JS_-} - \frac{\omega}{KS_-} \right]. \quad (21)$$

We solve the integrals for  $W_{\pm}$  using the residue theorem. This time the natural frequencies combine as  $v/J \pm \omega/K$  which are Lorentzian distributed with spread  $\tilde{\Delta} \equiv \Delta_v/J + \Delta_\omega/K$ . Equations (12) and (13) reduce to  $S_{\pm} = H^*(i\tilde{\Delta}/S_{\pm})$  and so

$$S_{\pm} = \sqrt{1 - 2\tilde{\Delta}}, \quad (22)$$

which bifurcates from 0 at

$$2\tilde{\Delta} = 2 \left( \frac{\Delta_v}{J} + \frac{\Delta_\omega}{K} \right) = 1. \quad (23)$$

Figure 2(a) shows this critical curve in the  $(J, K)$  plane. Notice it intersects with the critical curve of the phase wave at a point  $J = K = 2(\Delta_v + \Delta_\omega)$ . This means the sync state may bifurcate from the async state directly, without passing through the phase [Fig. 3(b)], which occurs when  $J = K$ . In this special case, Eqs. (4) and (5) for  $\dot{\zeta}, \dot{\eta}$  decouple and  $W_{\pm}(t)$  may be solved for all  $t$  (see Ref. [52]). In the generic case  $J \neq K$ , however, the sync state bifurcates from the intermediate mixed state [Fig. 3(c)]. As is evident from Fig. 2(a), the point  $J = K = 2(\Delta_v + \Delta_\omega)$  is a tetracritical point, at which four phases (async, sync, phase wave, and mixed) meet. The appearance of the sync state can be considered as the separation of dense clusters of locked swarmalators with time-independent coordinates and dilute drifting swarmalators in  $(x, \theta)$  space. This phenomenon is qualitatively similar to motility induced phase separation observed in self-propelled particles and various microorganisms, see for example [58].

To back up these numerical tests of our results we performed four additional analyses. First, we rederive  $S_{\pm}$  using a microscopic, swarmalator-level, approach (as opposed to the macroscopic, density-level approach the OA ansatz is based on). In the phase wave  $(S, 0)$ , swarmalators are partially locked in  $\dot{\zeta}_i = 0$  and drift in  $\dot{\eta}_i \neq 0$ . Applying these conditions to Eqs. (4) and (5) yields

$$\sin(\zeta_i - \Phi_+) = \frac{v_i + \omega_i}{S_+ J_+}, \quad (24)$$

$$\eta_i(t) = \eta_i(0) + \frac{1}{J_+} (Kv_i - J\omega_i)t, \quad (25)$$

where  $-S_+ J_+ \leq v_i + \omega_i \leq S_+ J_+$  and  $\eta_i(0)$  is an initial phase. Following Kuramoto [2], the order parameter must be self-consistent:  $S_+ := N^{-1} \sum_j e^{i\zeta_j}$ . Plugging Eq. (24) indeed gives the expression Eq. (19) for  $S_+$  in agreement with the generalized OA ansatz [similarly, Eq. (25) implies  $S_- = 0$  as expected]. We also attempted a microscopic analysis of the sync state but the calculations were beyond the scope of this Letter [52]. Second, we checked the identical swarmalator limit which has been analyzed previously (without an OA ansatz) [50]. As  $\Delta_v, \Delta_\omega \rightarrow 0$ , the critical curve for the phase wave Eq. (20) approaches  $J + K = 0$ , while that of the sync state Eq. (23) approaches  $J, K > 0$ , 0 in agreement with [50]. Figure 2(b) plots these in  $(J, K)$  space to allow a visual comparison. Third, we calculated the stability of async using the OA equations [Eqs. (10) and (11)] and found it agreed with Eq. (14) [52] (derived by perturbing the continuity equation [52]). Fourth, we used the OA equations to derive  $S_{\text{sync}}$  and its

critical coupling  $K_c$  for a simpler distribution  $g_{\omega(v)}(x) = (1/2)\delta(x - \Delta) + (1/2)\delta(x + \Delta)$  which agreed with simulation perfectly [52]. This completes our analysis.

“Hidden” phase transition.—We close by pointing out a curious feature of the swarmalator model. At  $J = 0$ , the positions evolves at constant speed  $\dot{x}_i = v_i \Rightarrow x_i = v_i t$  which means the phases obey

$$\dot{\theta}_i = \omega_i + \frac{K}{N} \sum_{j=1}^N \sin(\theta_j - \theta_i) \cos[(v_j - v_i)t]. \quad (26)$$

One can think of this equation as a model for a group of oscillators with random, time-dependent couplings. In turn, the results presented in this Letter reveal a phase transition hidden in the time dependence of  $\theta_i$ , which extends to the case where  $J = 0$ . This hidden phase transition causes incoherent oscillators to become phase locked at  $\theta_i = -v_i t + \zeta_i/2$  [the  $(S, 0)$  state] or  $\theta_i = v_i t - \eta_i/2$  [the  $(0, S)$ ], where  $\zeta_i$  ( $\eta_i$ ) is the phase from Eq. (26). Curiously, if we reinterpret  $v_i t$  as a heterogeneous field acting on the couplings, we see that the oscillators have become tuned to the field frequency  $v_i$ . To the best of our knowledge, this is a novel result and may provide a useful means for tuning a population of oscillators to a prescribed set of frequencies in an experimental setting.

To conclude, we have presented a simple, solvable model of swarmalators. The model has a rich phase diagram with a *tetracritical* point at which four phases meet. The model also captures the behavior of real-world swarmalators and active matter such as groups of sperm [59] and vinegar eels [60,61] (which swarm in quasi-1D rings), and the rotational component of 2D, real-world swarmalators such as forced colloids [11,12,14]. Our simulations showed that the cutoff in the spatial interaction kernel does not qualitatively change the dynamics of swarmalators in comparison to global coupling [52]. Thus, the exact solution of the swarmalator model with all-to-all coupling should have applicability to a variety of situations with local coupling. We hope our Letter will be useful to the active matter community, as it provides a new toy model, and interesting to the sync community, as the first OA ansatz for oscillators which are mobile (mobile in a 1D periodic domain, at least).

Future Letter could study the stability of the phase wave, mixed, and sync states (note we derived criteria for their *existence* only). Incorporating delayed interactions or external forcing—which are analyzable with our OA ansatz—would also be interesting. Finally, our model and predictions could be experimentally tested in circularly confined colloids or robotic swarms [36,37].

The code used in the simulations for this Letter is openly available from the Github repository [62].

This work is funded by national funds (OE) through Portugal’s FCT Fundação para a Ciência e Tecnologia,

I.P., within the scope of the framework contract foreseen in paragraphs 4, 5, and 6 of article 23, of Decree-Law 57/2016, of August 29, and amended by Law 57/2017, of July 19.

- 
- [1] Arthur T. Winfree, *The Geometry of Biological Time* (Springer Science & Business Media, New York, 2001), Vol. 12, [10.1007/978-1-4757-3484-3](https://doi.org/10.1007/978-1-4757-3484-3).
  - [2] Yoshiki Kuramoto, *Chemical Oscillations, Waves, and Turbulence* (Springer-Verlag, Berlin, Heidelberg, New York and Tokyo, 1984), [10.1007/978-3-642-69689-3](https://doi.org/10.1007/978-3-642-69689-3).
  - [3] Arkady Pikovsky, Jürgen Kurths, Michael Rosenblum, and Jürgen Kurths, *Synchronization: A Universal Concept in Nonlinear Sciences* (Cambridge University Press, Cambridge, England, 2003).
  - [4] Ziping Jiang and Martin McCall, Numerical simulation of a large number of coupled lasers, *J. Opt. Soc. Am. B* **10**, 155 (1993).
  - [5] Charles S. Peskin, *Mathematical Aspects of Heart Physiology* (Courant Institute of Mathematical Sciences, New York, 1975), pp. 268–278.
  - [6] William Bialek, Andrea Cavagna, Irene Giardina, Thierry Mora, Edmondo Silvestri, Massimiliano Viale, and Aleksandra M. Walczak, Statistical mechanics for natural flocks of birds, *Proc. Natl. Acad. Sci. U.S.A.* **109**, 4786 (2012).
  - [7] Yael Katz, Kolbjørn Tunstrøm, Christos C. Ioannou, Cristián Huepe, and Iain D. Couzin, Inferring the structure and dynamics of interactions in schooling fish, *Proc. Natl. Acad. Sci. U.S.A.* **108**, 18720 (2011).
  - [8] Ikkyu Aihara, Takeshi Mizumoto, Takuma Otsuka, Hiromitsu Awano, Kohei Nagira, Hiroshi G. Okuno, and Kazuyuki Aihara, Spatio-temporal dynamics in collective frog choruses examined by mathematical modeling and field observations, *Sci. Rep.* **4**, 3891 (2014).
  - [9] Kaiichiro Ota, Ikkyu Aihara, and Toshio Aoyagi, Interaction mechanisms quantified from dynamical features of frog choruses, *R. Soc. Open Sci.* **7**, 191693 (2020).
  - [10] Tzer Han Tan, Alexander Mietke, Hugh Higinbotham, Junang Li, Yuchao Chen, Peter J. Foster, Shreyas Gokhale, Jörn Dunkel, and Nikta Fakhri, Development drives dynamics of living chiral crystals, *Nature (London)* **607**, 287 (2022).
  - [11] Jing Yan, Moses Bloom, Sung Chul Bae, Erik Luijten, and Steve Granick, Linking synchronization to self-assembly using magnetic Janus colloids, *Nature (London)* **491**, 578 (2012).
  - [12] Jing Yan, Sung Chul Bae, and Steve Granick, Rotating crystals of magnetic Janus colloids, *Soft Matter* **11**, 147 (2015).
  - [13] Sangyeul Hwang, Trung Dac Nguyen, Srijanani Bhaskar, Jaewon Yoon, Marvin Klaiber, Kyung Jin Lee, Sharon C. Glotzer, and Joerg Lahann, Cooperative switching in large-area assemblies of magnetic Janus particles, *Adv. Funct. Mater.* **30**, 1907865 (2020).
  - [14] Bo Zhang, Andrey Sokolov, and Alexey Snezhko, Reconfigurable emergent patterns in active chiral fluids, *Nat. Commun.* **11**, 1 (2020).

- [15] Antoine Bricard, Jean-Baptiste Caussin, Debasish Das, Charles Savoie, Vijayakumar Chikkadi, Kyohei Shitara, Oleksandr Chepizhko, Fernando Peruani, David Saintillan, and Denis Bartolo, Emergent vortices in populations of colloidal rollers, *Nat. Commun.* **6**, 7470 (2015).
- [16] Bo Zhang, Hamid Karani, Petia M. Vlahovska, and Alexey Snezhko, Persistence length regulates emergent dynamics in active roller ensembles, *Soft Matter* **17**, 4818 (2021).
- [17] Raj Kumar Manna, Oleg E. Shklyaev, and Anna C. Balazs, Chemical pumps and flexible sheets spontaneously form self-regulating oscillators in solution, *Proc. Natl. Acad. Sci. U.S.A.* **118**, e2022987118 (2021).
- [18] Menglin Li, Martin Brinkmann, Ignacio Pagonabarraga, Ralf Seemann, and Jean-Baptiste Fleury, Spatiotemporal control of cargo delivery performed by programmable self-propelled Janus droplets, *Commun. Phys.* **1**, 1 (2018).
- [19] Kundan Chaudhary, Jaime J. Juárez, Qian Chen, Steve Granick, and Jennifer A. Lewis, Reconfigurable assemblies of Janus rods in ac electric fields, *Soft Matter* **10**, 1320 (2014).
- [20] Chao Zhou, Nobuhiko Jessis Suematsu, Yixin Peng, Qizhang Wang, Xi Chen, Yongxiang Gao, and Wei Wang, Coordinating an ensemble of chemical micromotors via spontaneous synchronization, *ACS Nano* **14**, 5360 (2020).
- [21] Mario Urso, Martina Ussia, and Martin Pumera, Breaking polymer chains with self-propelled light-controlled navigable hematite microrobots, *Adv. Funct. Mater.* **31**, 2101510 (2021).
- [22] Jia Dai, Xiang Cheng, Xiaofeng Li, Zhisheng Wang, Yufeng Wang, Jing Zheng, Jun Liu, Jiawei Chen, Changjin Wu, and Jinyao Tang, Solution-synthesized multifunctional Janus nanotree microswimmer, *Adv. Funct. Mater.* **31**, 2106204 (2021).
- [23] Kumar Vikrant and Ki-Hyun Kim, Metal–organic framework micromotors: Perspectives for environmental applications, *Catal. Sci. Technol.* **11**, 6592 (2021).
- [24] Jan Tesař, Martina Ussia, Osamah Alduhaish, and Martin Pumera, Autonomous self-propelled MnO<sub>2</sub> micromotors for hormones removal and degradation, *Appl. Mater. Today* **26**, 101312 (2022).
- [25] Jinxing Li, Oleg E. Shklyaev, Tianlong Li, Wenjuan Liu, Henry Shum, Isaac Rozen, Anna C. Balazs, and Joseph Wang, Self-propelled nanomotors autonomously seek and repair cracks, *Nano Lett.* **15**, 7077 (2015).
- [26] Rui Cheng, Weijie Huang, Lijie Huang, Bo Yang, Leidong Mao, Kunlin Jin, Qichuan ZhuGe, and Yiping Zhao, Acceleration of tissue plasminogen activator-mediated thrombolysis by magnetically powered nanomotors, *ACS Nano* **8**, 7746 (2014).
- [27] Laliphat Manamanchaiyaporn, Xiuzhen Tang, Xiaohui Yan, and Yuanyi Zheng, Molecular transport of a magnetic nanoparticle swarm towards thrombolytic therapy, *IEEE Robot. Autom. Lett.* **6**, 5605 (2021).
- [28] Bruno Ventejou, Hugues Chaté, Raul Montagne, and Xiaqing Shi, Susceptibility of Orientationally Ordered Active Matter to Chirality Disorder, *Phys. Rev. Lett.* **127**, 238001 (2021).
- [29] Kevin P O’Keeffe, Hyunsuk Hong, and Steven H Strogatz, Oscillators that sync and swarm, *Nat. Commun.* **8**, 1504 (2017).
- [30] Seung-Yeal Ha, Jinwook Jung, Jeongho Kim, Jinyeong Park, and Xiongtao Zhang, Emergent behaviors of the swarmalator model for position-phase aggregation, *Math. Models Methods Appl. Sci.* **29**, 2225 (2019).
- [31] Dan Tanaka, General Chemotactic Model of Oscillators, *Phys. Rev. Lett.* **99**, 134103 (2007).
- [32] Zeng Tao Liu, Yan Shi, Yongfeng Zhao, Hugues Chaté, Xia-qing Shi, and Tian Hui Zhang, Activity waves and freestanding vortices in populations of subcritical quince rollers, *Proc. Natl. Acad. Sci. U.S.A.* **118**, e2104724118 (2021).
- [33] Masatomo Iwasa and Dan Tanaka, Dimensionality of clusters in a swarm oscillator model, *Phys. Rev. E* **81**, 066214 (2010).
- [34] Demian Levis, Ignacio Pagonabarraga, and Benno Liebchen, Activity induced synchronization: Mutual flocking and chiral self-sorting, *Phys. Rev. Res.* **1**, 023026 (2019).
- [35] Benno Liebchen and Demian Levis, Collective Behavior of Chiral Active Matter: Pattern Formation and Enhanced Flocking, *Phys. Rev. Lett.* **119**, 058002 (2017).
- [36] Agata Barciś, Michał Barciś, and Christian Bettstetter, Robots that sync and swarm: A proof of concept in ROS 2, in *Proceedings of the 2019 International Symposium on Multi-Robot and Multi-Agent Systems (MRS)* (IEEE, New York, 2019), pp. 98–104.
- [37] Agata Barciś and Christian Bettstetter, Sandbots: Robots that sync and swarm, *IEEE Access* **8**, 218752 (2020).
- [38] Hyun Keun Lee, Kangmo Yeo, and Hyunsuk Hong, Collective steady-state patterns of swarmalators with finite-cutoff interaction distance, *Chaos* **31**, 033134 (2021).
- [39] Hyunsuk Hong, Active phase wave in the system of swarmalators with attractive phase coupling, *Chaos* **28**, 103112 (2018).
- [40] Joao U.F. Lizarraga and Marcus A.M. de Aguiar, Synchronization and spatial patterns in forced swarmalators, *Chaos* **30**, 053112 (2020).
- [41] Kevin P. O’Keeffe, Joep H.M. Evers, and Theodore Kolokolnikov, Ring states in swarmalator systems, *Phys. Rev. E* **98**, 022203 (2018).
- [42] Seung-Yeal Ha, Jinwook Jung, Jeongho Kim, Jinyeong Park, and Xiongtao Zhang, A mean-field limit of the particle swarmalator model, *Kinet. Relat. Models* **14**, 429 (2021).
- [43] Kevin O’Keeffe and Hyunsuk Hong, Swarmalators on a ring with distributed couplings, *Phys. Rev. E* **105**, 064208 (2022).
- [44] Gourab K. Sar, Sayantan Nag Chowdhury, Matjaz Perc, and Dibakar Ghosh, Swarmalators under competitive time-varying phase interactions, *New J. Phys.* **24**, 043004 (2022).
- [45] Kevin O’Keeffe and Christian Bettstetter, A review of swarmalators and their potential in bio-inspired computing, in *Proc. SPIE 10982, Micro- and Nanotechnology Sensors, Systems, and Applications XI* (SPIE, 2019), Vol. 10982, pp. 109822E, 10.1117/12.2518682
- [46] Udo Schilcher, Jorge F. Schmidt, Arke Vogell, and Christian Bettstetter, Swarmalators with stochastic coupling and memory, in *Proceedings of the 2021 IEEE International Conference on Autonomic Computing and Self-Organizing Systems (ACSOS)* (IEEE, New York, 2021), pp. 90–99.

- [47] Tamás Vicsek, András Czirók, Eshel Ben-Jacob, Inon Cohen, and Ofer Shochet, Novel Type of Phase Transition in a System of Self-Driven Particles, *Phys. Rev. Lett.* **75**, 1226 (1995).
- [48] John Toner and Yuhai Tu, Flocks, herds, and schools: A quantitative theory of flocking, *Phys. Rev. E* **58**, 4828 (1998).
- [49] Edward Ott and Thomas M Antonsen, Low dimensional behavior of large systems of globally coupled oscillators, *Chaos* **18**, 037113 (2008).
- [50] Kevin O’Keeffe, Steven Ceron, and Kirstin Petersen, Collective behavior of swarmalators on a ring, *Phys. Rev. E* **105**, 014211 (2022).
- [51] The original Kuramoto model has “all-to-all” coupling  $K_{ij} = K$ .
- [52] See Supplemental Material at <http://link.aps.org/supplemental/10.1103/PhysRevLett.129.208002> for the stability of steady states and the effects of local coupling, which contains Refs. [50,53–56].
- [53] S. H. Strogatz and R. E. Mirollo, Stability of incoherence in a population of coupled oscillators, *J. Stat. Phys.* **63**, 613 (1991).
- [54] S. Yoon, M. Sorbaro Sindaci, A. V. Goltsev, and J. F. F. Mendes, Critical behavior of the relaxation rate, the susceptibility, and a pair correlation function in the Kuramoto model on scale-free networks, *Phys. Rev. E* **91**, 032814 (2015).
- [55] L. M. Childs and S. H. Strogatz, Stability diagram for the forced Kuramoto model, *J. Nonlinear Sci.* **18**, 043128 (2008).
- [56] Edward Ott and Thomas M. Antonsen, Long time evolution of phase oscillator systems, *Chaos* **19**, 023117 (2009).
- [57] In 2D this looks like a vortex, see Ref. [29]; that’s why we called it a “vortexlike” phase wave in the abstract.
- [58] Michael E. Cates and Julien Tailleur, Motility-induced phase separation, *Annu. Rev. Condens. Matter Phys.* **6**, 219 (2015).
- [59] Adama Creppy, Franck Plouraboué, Olivier Praud, Xavier Druart, Sébastien Cazin, Hui Yu, and Pierre Degond, Symmetry-breaking phase transitions in highly concentrated semen, *J. R. Soc. Interface* **13**, 20160575 (2016).
- [60] A. C. Quillen, A. Peshkov, Esteban Wright, and Sonia McGaffigan, Synchronized oscillations in swarms of nematode *Turbatrix aceti*, *Soft Matter* **18**, 1174 (2022).
- [61] A. C. Quillen, A. Peshkov, Esteban Wright, and Sonia McGaffigan, Metachronal waves in concentrations of swimming *Turbatrix aceti* nematodes and an oscillator chain model for their coordinated motions, *Phys. Rev. E* **104**, 014412 (2021).
- [62] K. O’Keeffe, Swarmalator code (Version 1.0.1), <https://github.com/Khev/swarmalators> (2017).